Original Article

Kidney Res Clin Pract 2023;42(3):325-339
pISSN: 2211-9132 • eISSN: 2211-9140
https://doi.org/10.23876/j.krcp.22.034

KIDNEY RESEARCH AND CLINICAL PRACTICE

# The flavonoid fisetin ameliorates renal fibrosis by inhibiting SMAD3 phosphorylation, oxidative damage, and inflammation in ureteral obstructed kidney in mice

**Ha Young Ju[1], Jongwan Kim[2,*], Sang Jun Han[1,*]**

[1]*Department of Biotechnology, College of Fisheries Sciences, Pukyong National University, Busan, Republic of Korea*
[2]*Department of Medical Laboratory Science, Dong-Eui Institute of Technology, Busan, Republic of Korea*

**Background:** Renal fibrosis is characterized by the accumulation of extracellular matrix and inflammatory cells and kidney dysfunction, which is a major pathway in the progression of chronic kidney disease (CKD). Accumulating evidence indicates that oxidative stress plays a critical role in the initiation and progression of CKD via proinflammatory and profibrotic signaling pathways. Fisetin (3,3',4',7-tetrahydroxyflavone) has biological activities including antioxidant, anti-inflammatory, and anti-aging effects. Therefore, we evaluated the antifibrotic effects of fisetin on unilateral ureteral obstruction (UUO)-induced kidneys.

**Methods:** C57BL/6 female mice were subjected to right UUO and intraperitoneally injected every other day with fisetin (25 mg/kg/day) or vehicle from 1 hour before surgery to 7 days after surgery. Kidney samples were analyzed for renal fibrosis (α-smooth muscle actin [α-SMA] expression, collagen deposition, and transforming growth factor [TGF] β1/SMAD3 signaling pathway), oxidative damage (4-HNE and 8-OHdG expression), inflammation (proinflammatory cytokine/chemokine, macrophage, and neutrophil infiltration), and apoptosis (TUNEL staining). Cultured human proximal tubule cells were treated with fisetin before TGF-β to confirm the TGF-β downstream pathway (SMAD2/3 phosphorylation).

**Results:** We found that fisetin treatment protected against renal fibrosis by inhibiting the phosphorylation of SMAD3, oxidative damage, inflammation, apoptotic cell death, and accumulation of profibrotic M2 macrophages in the obstructed kidneys. In cultured human proximal tubular cells, fisetin treatment inhibited TGF-β1–induced phosphorylation of SMAD3 and SMAD2.

**Conclusion:** Fisetin alleviates kidney fibrosis to protect against UUO-induced renal fibrosis, and could be a novel therapeutic drug for obstructive nephropathy.

**Keywords:** Antioxidants, Chronic kidney diseases, Fisetin, Inflammation, Kidney fibrosis, Ureteral obstruction

**Received:** February 15, 2022; **Revised:** June 17, 2022; **Accepted:** June 28, 2022

**Correspondence:** Sang Jun Han
Department of Biotechnology, College of Fisheries Sciences, Pukyong National University, 45 Yongso-ro, Nam-gu, Busan 48513, Republic of Korea.
E-mail: sjhan@pknu.ac.kr
ORCID: https://orcid.org/0000-0002-5425-9056

Jongwan Kim
Department of Medical Laboratory Science, Dong-Eui Institute of Technology, 54 Yangji-ro, Busanjin-gu, Busan 47230, Republic of Korea.
E-mail: dahyun@dit.ac.kr
ORCID: https://orcid.org/0000-0001-6183-3100

*Sang Jun Han and Jongwan Kim contributed equally to this study as co-corresponding authors.

## Introduction

Renal fibrosis is a prominent feature of chronic kidney disease (CKD) progression. CKD is a critical kidney disease that can lead to end-stage renal disease (ESRD), which is defined as the complete loss of kidney function. Patients with ESRD are currently treated with therapies such as kidney transplants and hemodialysis [1]. Although many studies have been conducted on renal fibrosis, an effective treatment for renal fibrosis has not yet been established. Therefore, there is an urgent need to develop antifibrotic strategies to prevent renal fibrosis and treat CKD.

Fibrosis is characterized by the marked accumulation of extracellular matrix (ECM) in the tubulointerstitial space. This phenomenon occurs from various events, including fibroblast activation, interstitial macrophage infiltration, and activation of signaling factors such as transforming growth factor β (TGF-β) [1]. As a pathogenic factor, TGF-β1 is a major mediator of fibrosis development. TGF-β1/SMAD3 signaling is a key pathway regulating the initiation and progression of renal fibrosis. Upon exposure to stimuli such as reactive oxygen species (ROS), TGF-β1 phosphorylates intercellular signaling factors such as SMAD2/3; the activated SMAD complex enters the nucleus to transcribe genes involved in myofibroblast activation and matrix deposition. Various studies have suggested that myofibroblasts that produce ECM in the kidney are derived from several sources, such as epithelial cells, macrophages, endothelial cells, and resident fibroblasts through the TGF-β1/SMAD3 pathway [2,3].

Although there are various etiologies of renal damage in obstructive nephropathy, accumulating evidence indicates that oxidative stress caused by ROS plays a critical role. Increased ROS causes tubular epithelial cell death and damage to cellular macromolecules, including DNA, proteins, and lipids. In addition, ROS promotes the infiltration of inflammatory cells that release proinflammatory cytokines and chemokines [4]. Infiltrating inflammatory cells contribute to the maintenance and enhancement of the inflammatory response, as well as the stimulation of fibrogenic, apoptotic, and gene regulatory signaling pathways such as TGF-β, nuclear factor-kappa B (NF-κB), and the mitogen-activated protein kinase pathways [5].

Flavonoids have received substantial attention as medications and health food supplements because of their prospective therapeutic pharmacological and nutritional properties. Fisetin (3,3',4',7 tetrahydroxyflavone) is a flavonoid that is isolated from various seaweeds, fruits, and vegetables, including strawberries, apples, persimmons, and onions [6]. Studies reported that fisetin has biological activities including antioxidant [7], anti-inflammatory [8], and anticancer [9] effects. Sahu et al. [10] demonstrated that fisetin exhibited renoprotective effects by alleviating oxidative stress and apoptosis in renal tubular cells and regulating NF-κB activation in a cisplatin-induced nephrotoxicity model. Ren et al. [11] also demonstrated that fisetin protects against hyperuricemic nephropathy by modulating the STAT3 and β1/SMAD3 signaling pathway. However, the effect of fisetin on the progression of renal fibrosis and the underlying pathogenic mechanisms, with potential involvement of TGF-β1/SMAD3, ROS, inflammation, and renal tubular cell death, remain to be elucidated.

In this study, we investigated whether fisetin protects against renal fibrosis by regulating the TGF-β1/SMAD3 signaling pathway and by attenuating oxidative stress, inflammation, and cell death in mice with unilateral ureteral obstruction (UUO), a representative model of CKD.

## Methods

### Animals and establishment of the unilateral ureteral obstruction model

Female C57BL6 mice (8–12 weeks old) weighing 18–21 g were used for experiments. The mice were provided free access to water and standard chow. All animal surgeries were approved by the Institutional Animal Care and Use Committee of Pukyong National University (No. PKNUI-ACUC-2021-49) and were conducted in accordance with the Guide for the Care and Use of Laboratory Animals published by the US National Institutes of Health (NIH Publication No. 85–23, revised 2011).

All mice were anesthetized with pentobarbital sodium (50 mg/kg or to effect; Hanlim Pharma Co.) intraperitoneally before the operation. The mice were subjected to right UUO, as previously described [12]. Briefly, to induce ureteral obstruction, the right kidney was exposed via flank incision, the right ureter was completely tied with a 6-0 silk thread, and the incision was sutured. The left kidney was used as the control. The body temperature was maintained

at 36.5–37 °C during surgery and before and after anesthesia using a surgical heating pad (FHC, Inc.). The animals were divided into two groups: one group was intraperitoneally injected with fisetin (25 mg/kg; Pytolab; n = 5) 1 hour before surgery and on days 2, 4, and 6 after surgery and the second group received vehicle (n = 5) at the same time points. The concentration of fisetin was selected based on previous studies [13–15]. All mice were sacrificed 7 days after the surgery. Harvested kidneys were frozen in liquid nitrogen or fixed in 4% paraformaldehyde for subsequent analysis.

### Human proximal tubule cell culture

HK-2 cells, a human proximal tubular cell line, were purchased from the Korean Cell Line Bank. The cells were cultured in Dulbecco's modified Eagle's medium (Corning)–Ham's F12 (Welgene, Inc.) supplemented with 10% fetal bovine serum (MP Biomedicals) at 37 °C in a humidified 5% $CO_2$ incubator. After 16 hours of serum deprivation, cells were treated with 10 ng/mL human recombinant TGF-β for 30 minutes. In some experiments, cells were pretreated with 40 μM fisetin (n = 3) or vehicle (n = 3) 1 hour before TGF-β treatment.

### Western blotting

Kidney tissues were lysed and homogenized using the radioimmunoprecipitation assay lysis buffer (50 mM Tris-HCl, pH 8.0, 1% Triton-X 100, 0.5% sodium deoxycholate, 0.1% sodium dodecyl sulfate [SDS], 1 M NaF plus protease inhibitor cocktail [Sigma-Aldrich] and phosphatase inhibitor cocktail [Sigma-Aldrich]). Extracted protein samples were separated by SDS-PAGE and transferred to a polyvinylidene difluoride membrane (GVS S.p.A.). After blocking with 5% bovine serum albumin or skim milk for 30 minutes, the membranes were incubated with antibodies against α-smooth muscle actin (α-SMA, 1:20,000; Sigma-Aldrich), phosphorylated SMAD3 (p-SMAD3, 1:2,000; Abcam), p-SMAD2 (1:2,000; Abcam), t-SMAD 2/3 (1:2,000; Abcam), 4-hydroxynonenal (4-HNE, 1:2,000; Abcam), Ly6G (1:2,000; Fisher Scientific), and glyceraldehyde 3-phosphate dehydrogenase (GAPDH, 1:10,000; Bioworld Technology) overnight at 4 °C. The membranes were then treated for 1 hour at room temperature with horseradish peroxidase (HRP)-labeled goat anti-mouse immunoglobulin G (IgG, 1:3,000; Bethyl-Laboratories) or HRP-labeled goat anti-rabbit IgG (1:3,000; Bethyl-Laboratories). Total protein expression levels were normalized to GAPDH. Band intensities were analyzed using ImageJ software.

### Quantitative real-time polymerase chain reaction

Quantitative real-time (qRT) polymerase chain reaction (PCR) was performed to measure the messenger RNA (mRNA) expressions of markers of inflammation (monocyte chemoattractant protein-1 [MCP-1], macrophage inflammatory protein-2 [MIP-2], and interleukin-1β [IL-1β]), TGF-β1, and inducible nitric oxide synthase (iNOS) in the kidney after surgery. Total RNA was extracted from kidney tissues using TRIzol (Ambion) and synthesized as complementary DNA (cDNA) with random primers using reverse-transcription PCR. cDNA was measured by qRT-PCR (Bio-Rad) with the FastStart Universal SYBR Green Master Mix (Sigma-Aldrich) and primers (Table 1). mRNA levels were normalized to GAPDH mRNA. Relative expression was calculated using the cycle threshold method. Specificity was confirmed using melting curve analysis.

### Periodic acid-Schiff staining

The kidneys were fixed with 4% paraformaldehyde. Paraffin-embedded kidney tissue sections were stained with the periodic acid-Schiff (PAS) staining kit (Abcam) according to the manufacturer's protocol. To evaluate morphological damage to tubular cells, damage in a PAS-stained kidney section was scored in five fields in cortical areas per kidney using the following scoring method: 0, no damage; 1, mild damage with dilated tubular lumen; 2, moderate damage with flattened epithelial cells, dilated lumen, and congested lumen; and 3, severe damage with flat epithelial cells lacking nuclear staining and congested lumen [12].

### Masson's trichrome staining and Sirius red staining

Paraffin-embedded kidney tissue sections were stained using the Picro Sirius Red Stain Kit (Abcam) and Masson's trichrome stain. For picrosirius red staining, deparaffinized sections were covered completely with picrosirius red solution for 1 hour. The samples were then rinsed twice

**Table 1.** Primer sequences for the quantitative polymerase chain reaction analysis in this study

| Primer | Sequence (sense/antisense) | Annealing temperature (°C) |
|---|---|---|
| Mouse TGF-β1 | 5'-TTGTACGGCAGTGGCTGAAC-3' | 56 |
| | 5'-GGGCTGATCCCGTTGATTTC-3' | |
| Mouse MCP-1 | 5'-ACCTGCTGCTACTCATTCAC-3' | 60 |
| | 5'-TTGAGGTGGTTGTGGAAAAG-3' | |
| Mouse MIP-2 | 5'-CCAAGGGTTGACTTCAAGAAC-3' | 60 |
| | 5'-AGCGAGGCACATCAGGTACG-3' | |
| Mouse IL-1β | 5'-CTGAAAGCTCTCCACCTC-3' | 56 |
| | 5'-TGCTGATGTACCAGTTGGGG-3' | |
| Mouse iNOS | 5'-GCCTGTGAGACCTTTGATGTCC-3' | 66 |
| | 5'-CGGCTGGACTTTTCACTCTGC-3' | |
| Mouse GAPDH | 5'-ACCACAGTCCATGCCATCAC-3' | 65 |
| | 5'-CACCACCCTGTTGCTGTAGCC-3' | |

Annealing temperatures used for each primer are also provided.
GAPDH, glyceraldehyde 3-phosphate dehydrogenase; IL, interleukin; iNOS, inducible nitric oxide synthase; MCP-1, monocyte chemoattractant protein-1; MIP-2, macrophage inflammatory protein-2; TGF, transforming growth factor.

with acetic acid solution (Sigma-Aldrich). For Masson's trichrome staining, deparaffinized sections were refixed in Bouin's solution for 1 hour at 56 °C, and sections were stained in Weigert's iron hematoxylin working solution for 10 minutes. After washing, the sections were stained in Biebrich scarlet-acid fuchsin solution for 10 to 15 minutes, followed by staining in phosphomolybdic-phosphotungstic acid solution for 15 minutes. The picrosirius red or Masson's trichrome-stained sections were then continuously dehydrated in different concentrations of alcohol solutions. Finally, the sections were mounted on coverslips with Permount mounting medium (Fisher Scientific). Micrographs were taken randomly in 200× microscope image fields in cortical areas using a microscope (Leica DM2500; Leica Microsystems GmbH). Areas of collagen accumulation in the stained kidney tissues were analyzed using the ImageJ Fiji program.

### Immunohistochemical staining

Immunohistochemical (IHC) staining was performed to confirm the expression of α-SMA, which is a marker of fibrosis, infiltration of macrophages, and generation of 8-hydroxy-2'-deoxyguanosine (8-OhdG), an oxidized nucleoside of DNA. Paraffin-embedded kidney tissue sections were rehydrated, followed by antigen retrieval, peroxide quenching, and blocking. Sections were then incubated with primary antibodies in a humid chamber overnight at 4 °C. Primary antibodies against the following proteins were used for staining: mannose receptor (CD206, 1:200; Abcam), F4/80 (1:100; Bio-Rad), α-SMA (1:400; Sigma-Aldrich), and 8-OhdG (1:1,000; Abcam). Sections were then stained with HRP-conjugated goat anti-rat IgG or HRP-conjugated goat anti-mouse IgG (Bethyl-Laboratories). Hematoxylin was used to stain nuclei. The sections were observed using a Leica DM2500 microscope. Micrographs were taken randomly in 200× and 400× microscope image fields in the cortical areas. The α-SMA-, F4/80-, and 8-OhdG–positive cells were counted and recorded using the counting tool.

### Terminal deoxynucleotidyl transferase dUTP nick-end labeling assay

We performed terminal deoxynucleotidyl transferase dUTP nick-end labeling (TUNEL) staining using the DeadEnd Fluorometric TUNEL System Kit (Promega) according to the manufacturer's protocol. Briefly, kidney sections were deparaffinized and rehydrated. Next, the sections were incubated with the TUNEL reagent mixture for 1 hour at 37 °C and then washed with phosphate-buffered saline. Sections were mounted on coverslips with an antifade mounting medium. Images were obtained randomly at 200× microscope image fields in cortical areas under a Leica DM2500 microscope. TUNEL-positive cells were counted and recorded in five fields per kidney.

### Statistical analysis

Data were analyzed using the Student t test, one-way analysis of variance, and Tukey *post hoc* multiple comparison test. Results are expressed as the mean ± standard error of the mean. Statistical significance was set at $p < 0.05$.

## Results

### Fisetin alleviates unilateral ureteral obstruction-induced fibrosis in the kidney

First, we assessed the effect of fisetin on kidney fibrosis in obstructed kidneys in mice. Compared with controls, UUO-induced myofibroblast accumulation, which was characterized by increased expression of α-SMA (an activated fibrotic cell marker); western blotting also showed that treatment with fisetin significantly reduced the elevation of α-SMA ($p = 0.02$) (Fig. 1A, B). Moreover, the number of α-SMA–positive cells, as assessed by IHC staining, was upregulated in obstructed kidneys. Fisetin suppressed the upregulation of α-SMA–positive cells in renal tissues of UUO mice compared with that of vehicle-treated UUO mice (Fig. 1E, F). These results demonstrate that fisetin inhibits myofibroblast expansion in the fibrous kidney.

To further investigate the underlying mechanism, we examined whether fisetin affected activation of the TGF-β1/SMAD3 signaling pathways in UUO mice. A previous study shows that TGF-β1 served as a key mediator of fibrosis development and progression in CKD through SMAD3 phosphorylation [16]. Western blot analysis showed that p-SMAD3 expression was increased in the kidneys of mice subjected to UUO compared with that of mice in the control group and that fisetin notably blocked SMAD3 phosphorylation (Fig. 1A, C). However, there was no significant difference in TGF-β1 mRNA expression between vehicle-treated mice and fisetin-treated mice after UUO (Fig. 1D). Together, these results indicate that fisetin treatment may alleviate kidney fibrosis by inhibiting SMAD3 phosphorylation after UUO. To further examine the effect of fisetin on the TGF-β1/SMAD pathway, HK-2 cells, a human kidney epithelial cell line, were pretreated with 40 μM fisetin or vehicle 1 hour before treatment with 10 ng/mL TGF-β1. Western blot analysis showed that fisetin pretreatment significantly reduced the TGF-β1-induced phosphorylation of SMAD2 ($p = 0.03$) and SMAD3 ($p = 0.02$) in HK-2 cells compare with vehicle-treated cells (Fig. 1G–K).

### Fisetin reduces unilateral ureteral obstruction-induced collagen deposition in renal interstitial area

To examine the effects of fisetin on UUO-induced ECM accumulation, we analyzed collagen deposition using Sirius red staining and Masson's trichrome staining. Collagen deposition was increased in the interstitium after UUO, and this increase was significantly lower in the kidneys of fisetin-treated mice than in the kidneys of vehicle-treated mice ($p = 0.005$) (Fig. 2A). The quantified results indicated that the deposition of collagen in the interstitial area was notably elevated in mice subjected to UUO, while it was partially restored in mice treated with fisetin (Fig. 2B, C).

### Fisetin protects against renal damage and tubule cell apoptosis after unilateral ureteral obstruction

We analyzed the effect of fisetin on renal tubular injury after UUO using PAS staining. The obstructed kidneys of UUO mice exhibited severe structural disorders characterized by tubular dilation and atrophy, as well as luminal congestion. In contrast, obstructed kidneys of mice treated with fisetin showed significantly less luminal congestion and tubular dilation and atrophy compared with the obstructed kidneys of vehicle-treated mice, indicating that fisetin treatment ameliorated the UUO-induced renal morphological damage (Fig. 3A). The renal damage score (scale, 0–3) for histological grading was used to measure the extent of renal tubular damage after UUO. Fisetin-treated mice subjected to UUO had significantly lower renal damage scores than vehicle-treated mice after UUO ($p < 0.001$) (Fig. 3B). We then investigated whether fisetin treatment showed an effect on renal tubular apoptosis after UUO. UUO increased the number of TUNEL-positive tubule cells, and this increase was lower in fisetin-treated mice than in vehicle-treated mice (Fig. 3A, C). These results demonstrate that fisetin treatment protects against UUO-induced renal tubular damage and apoptosis of tubule cells.

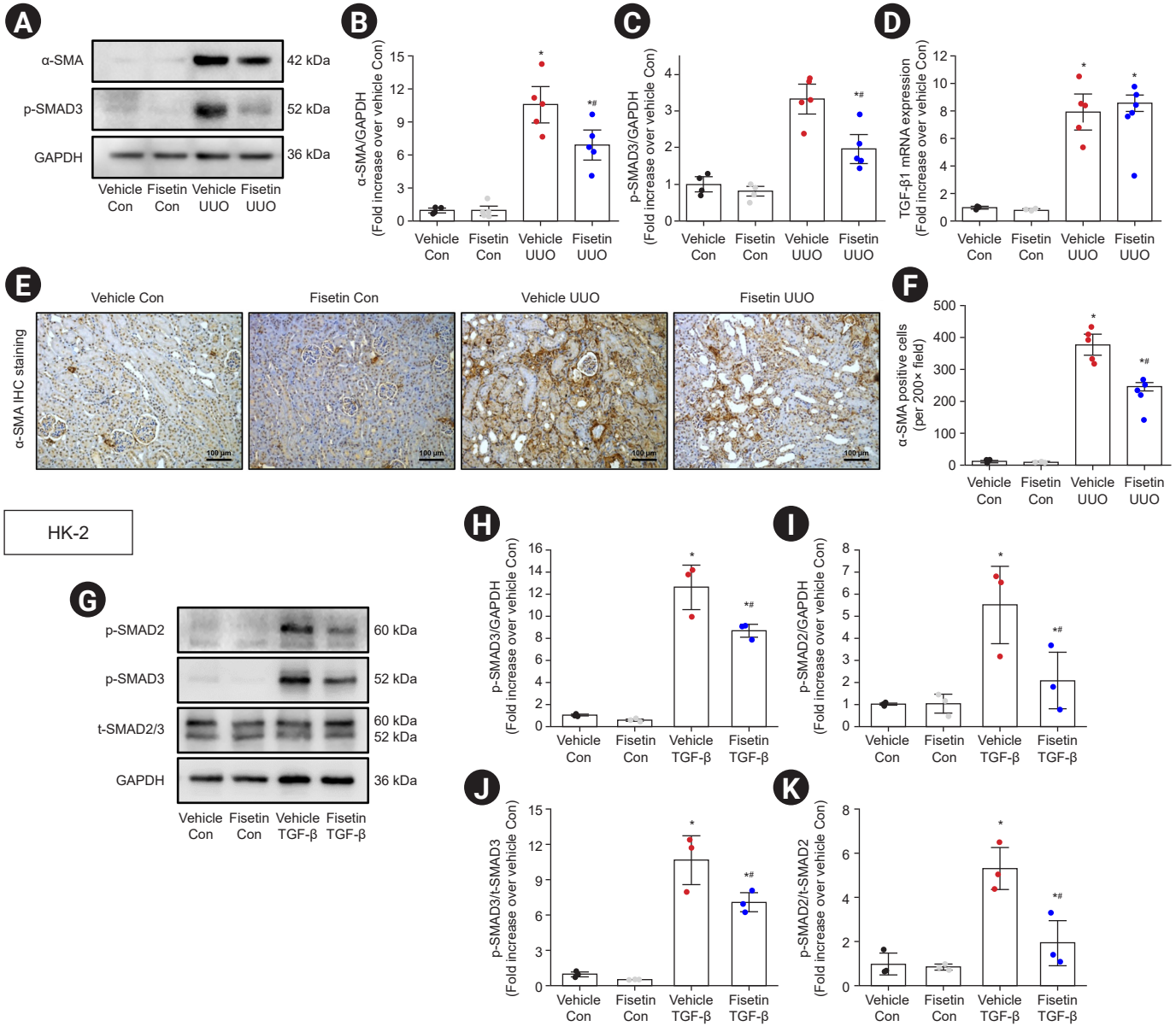


**Figure 1. Effect of fisetin on myofibroblast expansion and the TGF-β/SMAD3 signaling pathway in ureteral obstructed kidneys and TGF-β1-treated HK-2 cells.** Mice were subjected to right UUO and treated with fisetin or vehicle. Seven days after surgery, kidney samples were harvested for western blotting using α-SMA and p-SMAD3 antibodies (A), which are markers of fibrosis. GAPDH was used as a loading control. (B, C) Band densities of α-SMA and p-SMAD3 were measured using ImageJ software. (D) TGF-β1 mRNA expression was measured using quantitative real-time polymerase chain reaction. (E) Representative images of kidney sections subjected to immunohistochemical staining using an α-SMA antibody. Hematoxylin was used to visualize the nuclei of cells. (F) The number of α-SMA in the interstitial area is shown. HK-2 cells were pretreated with 40-μM fisetin or vehicle for 1 hour, followed by TGF-β treatment for 30 minutes. (G) HK-2 cells (n = 3) were subjected to western blotting using p-SMAD3, p-SMAD2, and t-SMAD2/3 antibodies. GAPDH was used as a loading control. (H, I) Band densities of p-SMAD3 and p-SMAD2 were measured using ImageJ software. (J, K) The ratio of p-SMAD3 and p-SMAD2 to t-SMAD2/3 was calculated. Results were expressed as the mean ± standard error of the mean (vehicle or fisetin control, n = 4; vehicle or fisetin UUO, n = 5). One-way analysis of variance plus Tukey *post hoc* multiple comparison test was used to detect significant changes.

α-SMA, α-smooth muscle actin; Con, control; GAPDH, glyceraldehyde 3-phosphate dehydrogenase; IHC, immunohistochemical; mRNA, messenger RNA; p-SMAD, phosphorylated SMAD; TGF, transforming growth factor; t-SMAD, total-SMAD; UUO, unilateral ureteral obstruction.

*$p < 0.05$ vs. vehicle control kidneys or vehicle-treated HK-2 cells, $^{\#}p < 0.05$ vs. vehicle UUO kidneys or TGF-β–treated HK-2 cells.

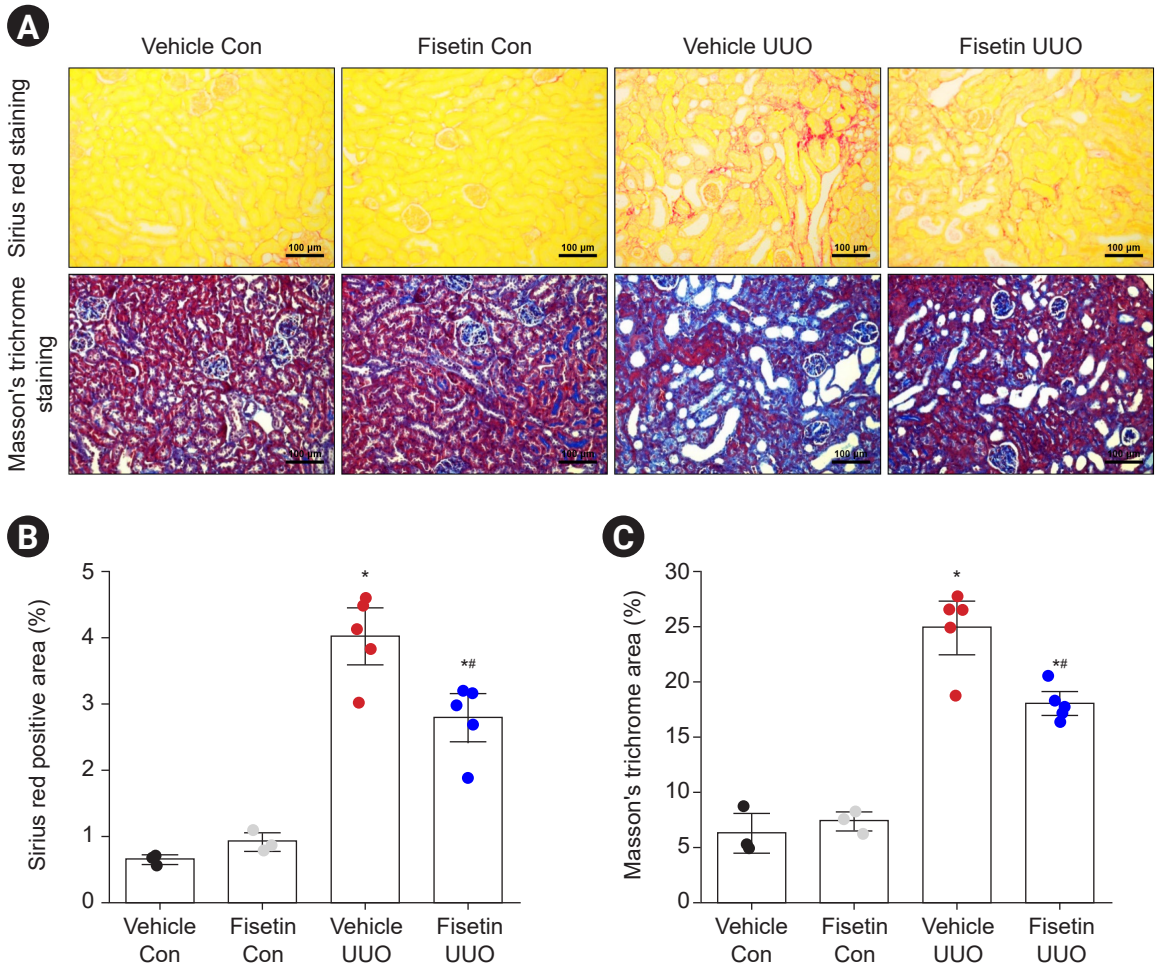


**Figure 2. Effect of fisetin on collagen deposition in ureteral obstructed kidneys.** Mice were subjected to right UUO and treated with fisetin or vehicle. Seven days after surgery, kidney sections were subjected to Sirius red staining and Masson trichrome staining. Representative images of kidney sections subjected to Sirius red (A, upper panel) and Masson trichrome staining (A, lower panel) are presented. (B, C) Collagen deposition was measured as described in the Methods section. Results were expressed as the mean ± standard error of the mean (vehicle or fisetin control, n = 3; vehicle or fisetin UUO, n = 5). One-way analysis of variance plus Tukey *post hoc* multiple comparison test was used to detect significant changes.
Con, control; UUO, unilateral ureteral obstruction.
*$p < 0.05$ vs. vehicle control, $^{\#}p < 0.05$ vs. vehicle UUO.

### Fisetin attenuates inflammation in obstructed kidneys after unilateral ureteral obstruction

Fig. 4A shows representative images of IHC staining for macrophages (dark brown) in the kidneys of each group of mice. Macrophage infiltration was significantly increased in the renal cortex of mice subjected to UUO. Fisetin-treated mice showed decreased macrophage infiltration in obstructed kidneys compared with that in vehicle-treated mice (Fig. 4A, B). Western blotting also showed that neutrophil expression was increased in vehicle-treated mice subjected to UUO. In addition, fisetin treatment significantly attenuated the levels of neutrophils in obstructed kidneys compared with vehicle treatment ($p = 0.03$) (Fig. 4C, D). Next, we examined the mRNA expression of proinflammatory cytokine and chemokines (MCP-1, MIP-2, and IL-1β) in the kidneys 7 days after UUO by qRT-PCR. MCP-1, MIP-2, and IL-1β mRNA expressions were remarkably increased in vehicle-treated mice subjected to UUO, and this induction was attenuated by fisetin treatment (Fig. 4E–G).

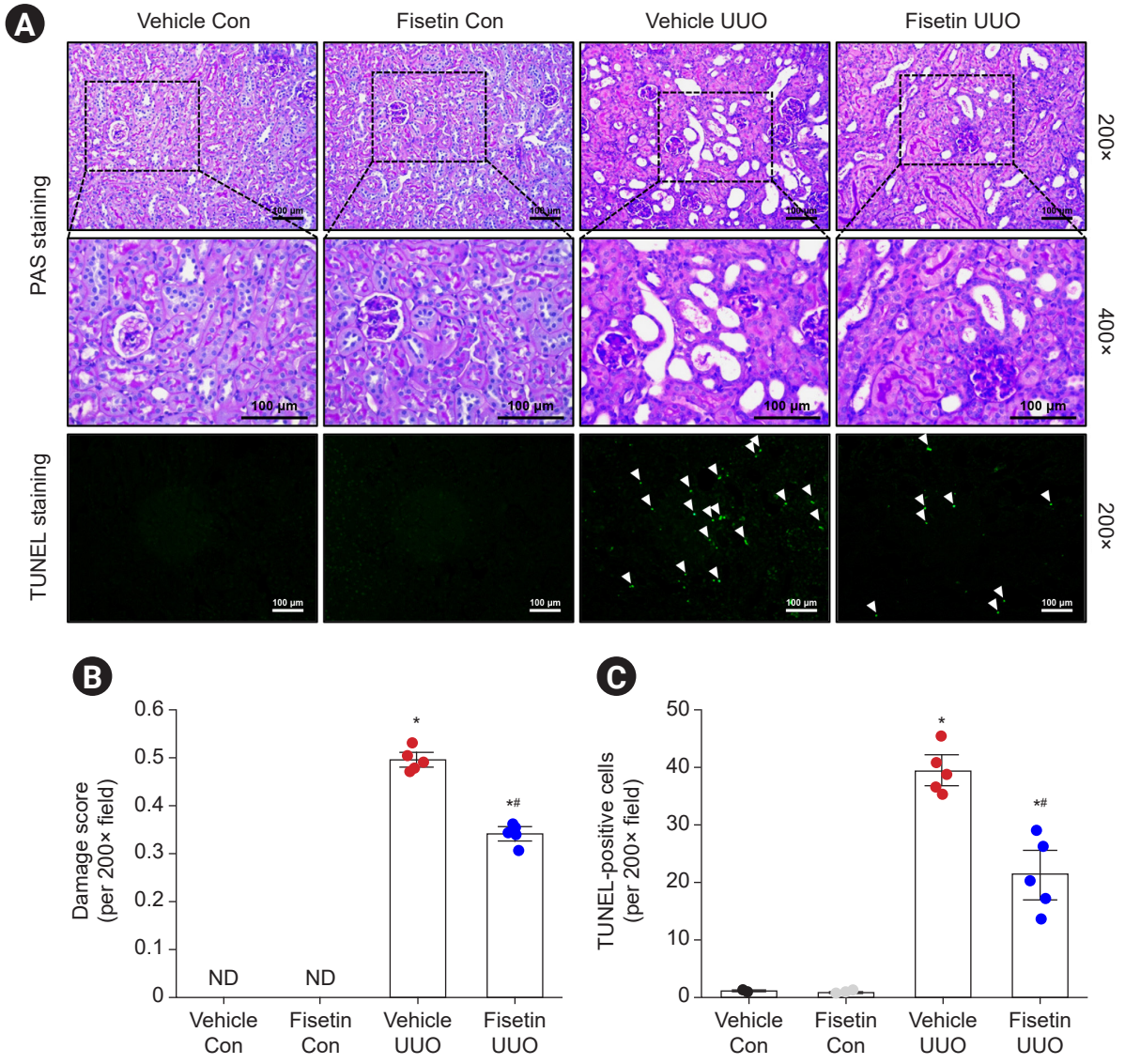


**Figure 3. Effects of fisetin on UUO-induced tubular damages and apoptotic tubular cell death.** Mice were subjected to right UUO and treated with fisetin or vehicle. Seven days after surgery, kidney sections were subjected to PAS staining and TUNEL staining. Images were obtained from the cortex. Representative images of kidney sections subjected to PAS staining (A: top panel, magnification ×200; middle panel, magnification ×400) are presented. (B) Kidney damage was scored as described in the Methods section. Representative images of kidney sections subjected to TUNEL assay (A, bottom panel) are presented. Images were obtained from the cortex. (C) TUNEL-positive cells were counted. Results were expressed as the mean ± standard error of the mean (vehicle or fisetin control, n = 3; vehicle or fisetin UUO, n = 5). The Mann-Whitney nonparametric test was used to detect significant changes in histological damage score and the one-way analysis of variance plus Tukey *post hoc* multiple comparison test was used to detect significant changes in TUNEL-positive cells.

ND, not detected; PAS, periodic acid-Schiff; TUNEL, terminal deoxynucleotidyl transferase dUTP nick-end labeling; UUO, unilateral ureteral obstruction.

*$p < 0.05$ vs. vehicle control, $^{\#}p < 0.05$ vs. vehicle UUO.

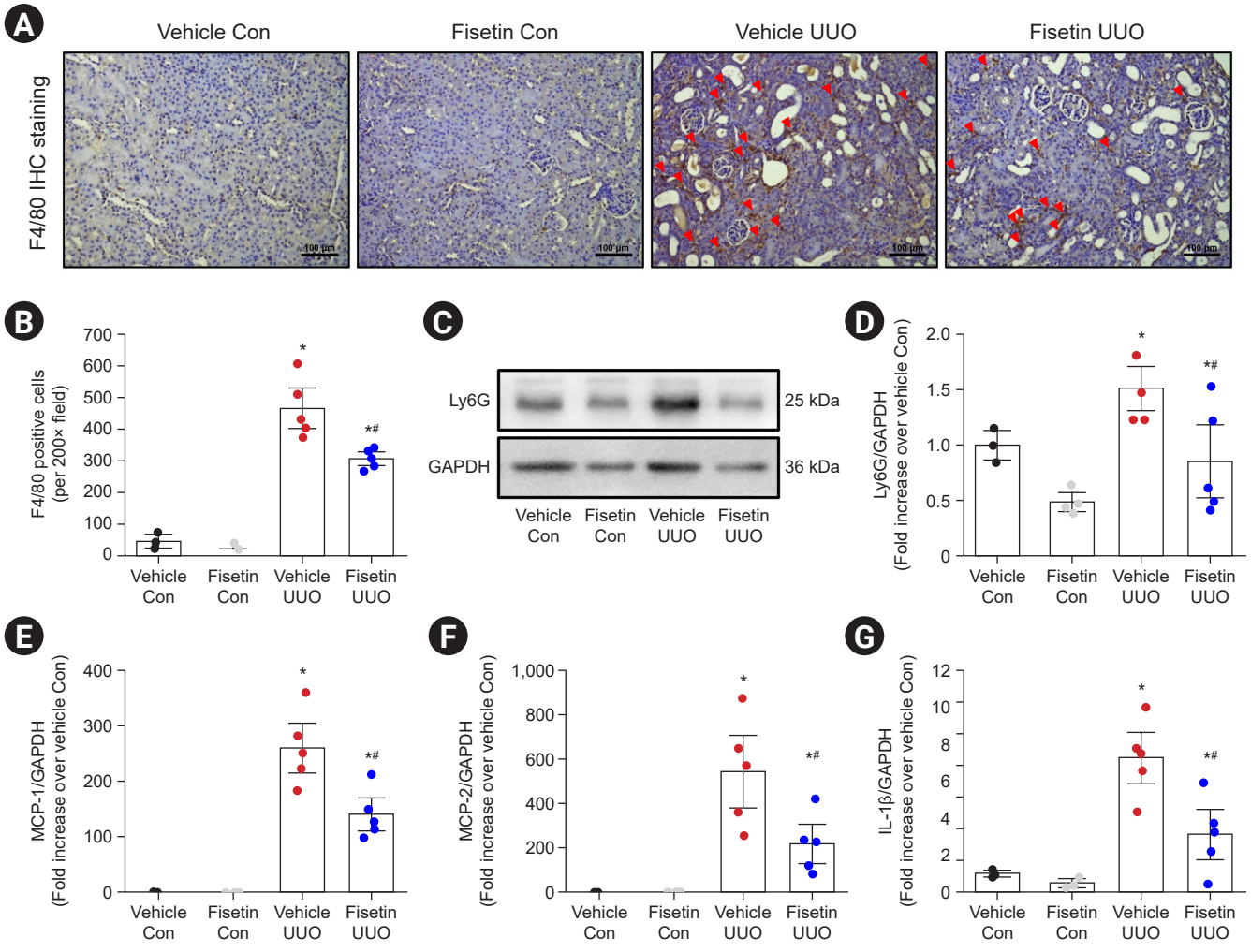


**Figure 4. Effect of fisetin on inflammatory cell infiltration and proinflammatory cytokines and chemokines synthesis in ureteral obstructed kidneys.** Mice were subjected to right UUO and treated with fisetin or vehicle. Seven days after surgery, kidney sections were subjected to immunohistochemistry staining using F4/80 antibody, which is a macrophage marker. Hematoxylin was used to visualize the nuclei of cells. (A) The representative images of F4/80 IHC staining and number of macrophages (B) are shown. (C) Kidney samples were subjected to western blotting using the Ly6G (a marker of neutrophil) antibody. GAPDH was used as a loading control. (D) Band densities were measured using the ImageJ software. The mRNA expressions of MIP-2 (E), MCP-1 (F), and IL-1β (G) were measured with quantitative real-time polymerase chain reaction. Each mRNA expression was normalized to GAPDH expression. Results were expressed as the mean ± standard error of the mean (vehicle or fisetin control, n = 3; vehicle or fisetin UUO, n = 5). One-way analysis of variance plus Tukey *post hoc* multiple comparison test was used to detect significant changes.
Con, control; GAPDH, glyceraldehyde 3-phosphate dehydrogenase; IHC, immunohistochemical; IL, interleukin; MCP-1, monocyte chemoattractant protein-1; MIP-2, macrophage inflammatory protein-2; mRNA, messenger RNA; UUO, unilateral ureteral obstruction.
*$p < 0.05$ vs. vehicle control, $^{\#}p < 0.05$ vs. vehicle UUO.

### Fisetin attenuates the accumulation of M2 macrophage in the obstructed kidneys after unilateral ureteral obstruction

M1 macrophages initiate an inflammatory response at the initial stage of injury and differentiate into profibrotic M2 macrophages as the injury progresses [17]. We demonstrated that fisetin attenuated renal inflammation in mice with UUO nephropathy (Fig. 4). Therefore, we examined the infiltration of M2 macrophage using CD206, a marker

of M2, and the mRNA expression of iNOS, a marker of M1. Fig. 5A shows representative images of IHC for M2 macrophages (dark brown) in the kidneys of each group of mice. M2 macrophage accumulation was significantly increased in the renal cortex of mice subjected to UUO. However, fisetin treatment decreased M2 macrophage accumulation in interstitial area of kidney compared with vehicle treatment in UUO group (Fig. 5A, B). In contrast, there was no difference in iNOS mRNA expression levels between the vehicle-treated groups and the fisetin-treated groups after UUO (Fig. 5C).

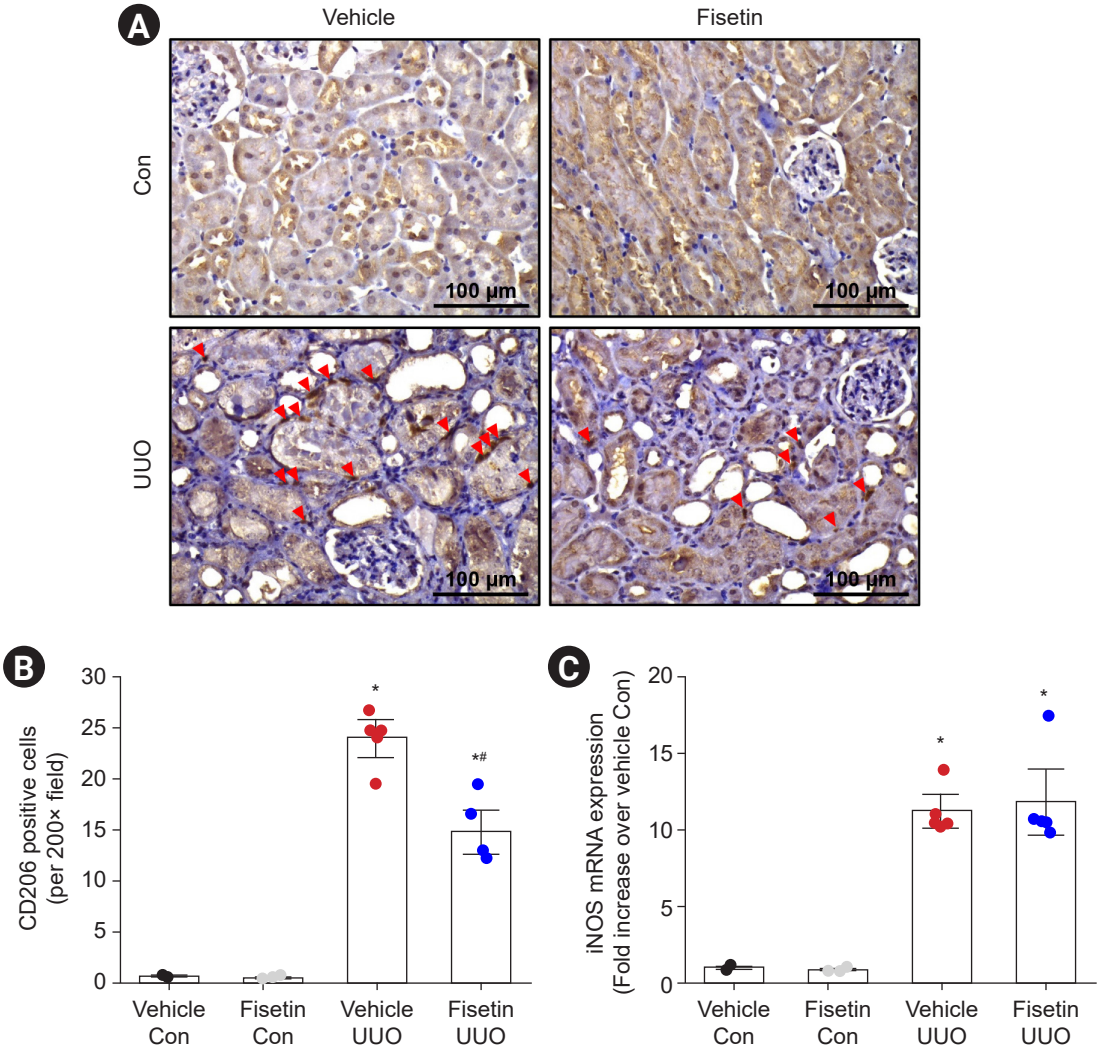


**Figure 5. Effect of fisetin on M1 and M2 macrophage expressions in ureteral obstructed kidneys.** Mice were subjected to right UUO and treated with fisetin or vehicle. Seven days after surgery, kidney sections were subjected to iimmunohistochemical staining using anti-CD206 antibody, which is an M2 macrophage marker. Hematoxylin was used to visualize the nuclei of cells. (A) The representative images of CD206 immunohistochemical; staining and number of CD206-positive cells (B) are shown. (C) The mRNA expressions of iNOS, an M1 macrophage marker, were analyzed by quantitative real-time polymerase chain reaction. Each mRNA expression was normalized to GAPDH expression. Results were expressed as the mean ± standard error of the mean (vehicle or fisetin control, n = 3; vehicle or fisetin UUO, n = 5). One-way analysis of variance plus Tukey *post hoc* multiple comparison test was used to detect significant changes.

Con, control; GAPDH, glyceraldehyde 3-phosphate dehydrogenase; iNOS, inducible nitric oxide synthase; mRNA, messenger RNA; UUO, unilateral ureteral obstruction.

*$p < 0.05$ vs. vehicle control, $^{\#}p < 0.05$ vs. vehicle UUO.

### Fisetin attenuates oxidative damage caused by oxidative stress after unilateral ureteral obstruction

We next assessed the effect of fisetin on oxidative damage in UUO mice. Fig. 6A shows representative images of IHC for 8-OHdG (dark brown) in the kidneys of each group of mice. The results showed that 8-OHdG expression was significantly increased in the renal cortex of mice subjected to UUO. In addition, fisetin treatment reduced the expression of 8-OHdG in obstructed kidneys compared to that in vehicle-treated mice (Fig. 6A–C). Western blotting also showed that the expression of 4-HNE, an indicator of lipid peroxidation, was significantly increased in kidneys after UUO, and this increase was lower in mice treated with fisetin compared to mice treated with vehicle (Fig. 6D, E).

## Discussion

In this study, we demonstrated, for the first time, that fisetin treatment effectively protects against UUO-induced renal fibrosis by decreasing ECM accumulation, oxidative damage, inflammation, and cell apoptosis. Obstructed kidneys show typical features of obstructive nephropathy, such as increased collagen deposition, tubular damage, infiltration of inflammatory cells, and tubular cell death [18]. In addition, the expression of α-SMA, a marker for activated myofibroblasts, was increased, which was also accompanied by an increase in SMAD3 phosphorylation after UUO.

TGF-β1/SMAD3 signaling is a major signaling pathway in the pathogenesis of tubulointerstitial fibrosis. TGF-β1 binds to TβRII, which activates TβRI, resulting in the activation of TGF-β1 downstream effectors [19]. The activated forms, p-SMAD2 and SMAD3 complexes with SMAD4, translocate into the nucleus and regulate the transcription of target fibrogenesis genes [20]. p-SMAD3 is a key factor in the transcription of fibrogenesis genes mediated by TGF-β1, leading to UUO-induced renal fibrosis [21]. As a result of confirming the expression level of p-SMAD3 and TGF-β1, we demonstrated that fisetin alleviates fibrosis by regulating the downstream effectors of TGF-β1 signaling based on the result that there was no significant difference in TGF-β1 mRNA expression between vehicle-treated mice and fisetin-treated mice after UUO. Fisetin treatment also dramatically suppressed SMAD3 phosphorylation in the UUO model. Furthermore, we also confirmed that fisetin significantly suppressed TGF-β–induced SMAD2/3 phosphorylation in cultured human kidney tubular cells. Based on these results, we speculate that fisetin treatment inhibited the phosphorylation of SMAD3, resulting in suppression of nuclear translocation of the SMAD complex and the expression of SMAD-mediated genes, resulting in reductions in α-SMA and collagen production rather than direct regulation of TGF-β1 expression. Another study reported that GQ5, a small molecular phenolic compound, attenuated renal fibrosis by selectively inhibiting TGF-β1 mediated SMAD3 phosphorylation [22]. MAF, a renin-angiotensin system inhibitor, attenuates epithelial-to-mesenchymal transition and interstitial fibrosis by selectively suppressing the TGF-β1–induced SMAD3 phosphorylation [23]. Moreover, fisetin has been reported to significantly inhibit SMAD3 phosphorylation in myocardial infarction-induced adverse atrial fibrosis [24] and bleomycin-induced pulmonary fibrosis [15] animal models. However, the underlying molecular mechanism of fisetin-regulated SMAD3 phosphorylation in a UUO model has not yet been defined.

Oxidative stress may be exacerbated by increased ROS production after UUO, and this oxidative stress contributes significantly to the pathogenesis of UUO [25]. In addition, ROS act as central molecules of inflammatory and apoptotic signaling, ultimately leading to cell death [26]. Modification of DNA, proteins, and lipids by oxidative stress has been shown to play important roles in many biological pathways, such as cell apoptosis and ECM expansion [27]. 8-OhdG is a product of oxidative damage to 2'-deoxyguanosine and is a ubiquitous marker for measuring oxidative DNA damage [28]. Meanwhile, reactive aldehyde 4-HNE is a major bioactive product of polyunsaturated fatty acids under oxidative stress and is used as an indicator of lipid oxidation [29]. We confirmed that fisetin significantly reduced HNE and 8-OhdG expression as well as tubular cell apoptosis in UUO mice. This indicates that fisetin treatment has a protective effect against renal damage by alleviating oxidative stress produced during UUO.

Interstitial myofibroblast accumulation and macrophage recruitment are associated with progression of renal injury in mice with obstructive nephropathy [30]. Macrophages secrete proinflammatory cytokines and chemokines, as well as growth factors such as TGF-β and fibroblast growth factor, leading to tissue injury and development of renal

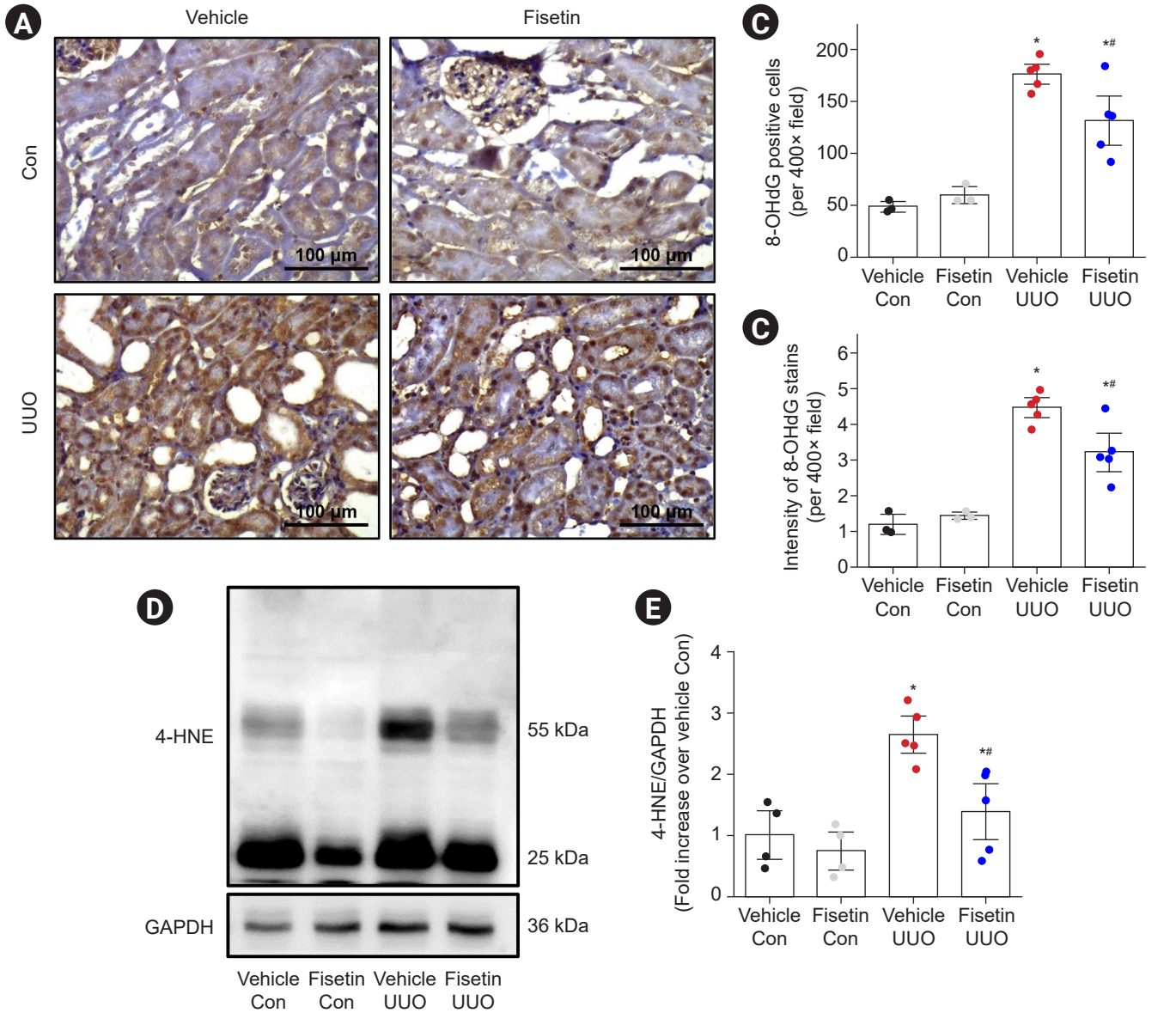


**Figure 6. Effect of fisetin on oxidative damage in ureteral obstructed kidneys.** Mice were subjected to right UUO and treated with fisetin or vehicle. Seven days after surgery, kidney sections were subjected to IHC staining using 8-OHdG (marker of damaged DNA) antibody. Hematoxylin was used to visualize the nuclei of cells. (A) Representative images of 8-OhdG IHC staining and number (B) and intensity (C) of 8-OhdG are shown. (D) Kidney samples were subjected to western blotting using an antibody against 4-HNE, which is an α, β-unsaturated hydroxyalkenal produced by lipid peroxidation. GAPDH was used as a loading control. (E) Band densities were measured using the ImageJ software. Results were expressed as the mean ± standard error of the mean (vehicle or fisetin control, n = 3; vehicle or fisetin UUO, n = 5). One-way analysis of variance plus Tukey *post hoc* multiple comparison test was used to detect significant changes. Con, control; GAPDH, glyceraldehyde 3-phosphate dehydrogenase; IHC, immunohistochemical; UUO, unilateral ureteral obstruction. 4-HNE, 4-hydroxynonenal; 8-OhdG, 8-hydroxy-2'-deoxyguanosine.
*$p < 0.05$ vs. vehicle control, $^{\#}p < 0.05$ vs. vehicle UUO.

fibrosis [31]. In this study, we found that proinflammatory cytokines and chemokines (MCP-1, MIP-2, and IL-1β) were increased in obstructed kidneys after UUO. MCP-1 and IL-1β promote the migration and infiltration of monocytes and macrophages, as well as the differentiation of monocytes into macrophages, whereas MIP-2 is produced by various

cell types such as macrophages, monocytes, and epithelial cells to recruit and activate neutrophils, thereby playing a key role in the inflammatory response [32–34]. In the present study, decreased expression of macrophage-recruiting cytokines (MCP-1, MIP-2, and IL-1β) and neutrophil expression in fisetin-treated mice are consistent with our finding that fisetin treatment significantly attenuated macrophage infiltration including profibrotic M2 macrophages after UUO compared to vehicle-treated mice. Furthermore, SMAD3 is a critical factor in macrophage/monocyte chemotaxis [21,35]. Inazaki et al. [21] also demonstrated that accumulation of renal interstitial inflammatory cells, such as macrophages, were remarkably suppressed by SMAD3 deficiency. M1 macrophages initiate an inflammatory response at the initial stage of injury and differentiate into M2 macrophages as injury progresses in obstructed kidneys [36]; in addition, M1 macrophage-producing or -recruiting chemokine/cytokine mRNA levels were higher in the vehicle-treated group than in fisetin-treated group after UUO. Consequently, we speculate that M1 macrophages showed more infiltration in the initial stage of injury in vehicle-treated UUO kidneys than in fisetin-treated UUO kidneys and that more M1 macrophages were differentiated into M2 macrophages in the vehicle-treated group than in the fisetin-treated group, so the amount of undifferentiated M1 macrophages in obstructed kidneys as evaluated by iNOS mRNA expression was similar the two groups at the end point of our experiments at the 7th day after UUO (the end point of our experiments).

In summary, we demonstrated that fisetin protects against obstructive nephropathy. We found that fisetin exhibits powerful antifibrotic effects in obstructed kidneys by inhibiting SMAD3 phosphorylation. However, previous studies showed that SMAD3 as well as other SMADs such as SMAD2 and SMAD4 are activated in the TGFβ1-mediated signaling pathway and regulate the transcription of fibrosis genes by interacting with each other. To confirm that fisetin alleviates fibrosis through SMAD3 phosphorylation, it is necessary to demonstrate that fisetin selectively and specifically inhibits SMAD3 by investigating the expression levels of other factors in the TGF-β1/SMAD3 signaling pathway. In addition, SMAD3 and SMAD2 are recruited to and phosphorylated by TβRI by adapter proteins such as SMAD anchor for receptor activation (SARA) upon TGF-β1 stimulation [37]. To elucidate the mechanism by which fisetin inhibits SMAD3 phosphorylation, further studies on these factors will be needed. Nonetheless, we clearly showed that fisetin treatment remarkably attenuated renal fibrosis, tubular damage, oxidative damage, inflammation, and apoptosis induced by UUO, suggesting that fisetin may be a potent inhibitor of TGF-β1/SMAD3 signaling, a major pathway in fibrosis, and may be a novel therapeutic drug for obstructive nephropathy.

## Conflicts of interest

All authors have no conflicts of interest to declare.

## Funding

This work was supported by a Research Grant of Pukyong National University (2020).

## Data sharing statement

The data presented in this study are available on request from the corresponding author.

## Authors' contributions

Conceptualization, Data curation: HYJ, SJH
Formal analysis, Investigation, Methodology: All authors
Resources, Supervision: SJH
Visualization: JK
Funding acquisition: SJH
Writing–original draft: All authors
Writing–review & editing: All authors
All authors read and approved the final manuscript.

## ORCID

Ha Young Ju, https://orcid.org/0000-0003-1019-0023
Jongwan Kim, https://orcid.org/0000-0001-6183-3100
Sang Jun Han, https://orcid.org/0000-0002-5425-9056

## References

1. Cho MH. Renal fibrosis. *Korean J Pediatr* 2010;53:735–740.
2. Shu DY, Lovicu FJ. Myofibroblast transdifferentiation: the dark force in ocular wound healing and fibrosis. *Prog Retin Eye Res*

2017;60:44–65.
3. Jang HS, Kim JI, Han SJ, Park KM. Recruitment and subsequent proliferation of bone marrow-derived cells in the postischemic kidney are important to the progression of fibrosis. *Am J Physiol Renal Physiol* 2014;306:F1451–F1461.
4. Chevalier RL, Forbes MS, Thornhill BA. Ureteral obstruction as a model of renal interstitial fibrosis and obstructive nephropathy. *Kidney Int* 2009;75:1145–1152.
5. Dendooven A, Ishola DA, Nguyen TQ, et al. Oxidative stress in obstructive nephropathy. *Int J Exp Pathol* 2011;92:202–210.
6. Pal HC, Pearlman RL, Afaq F. Fisetin and its role in chronic diseases. *Adv Exp Med Biol* 2016;928:213–244.
7. Zhang H, Zheng W, Feng X, et al. Nrf2–ARE signaling acts as master pathway for the cellular antioxidant activity of fisetin. *Molecules* 2019;24:708.
8. Park HH, Lee S, Oh JM, et al. Anti-inflammatory activity of fisetin in human mast cells (HMC-1). *Pharmacol Res* 2007;55:31–37.
9. Sun X, Ma X, Li Q, et al. Anti-cancer effects of fisetin on mammary carcinoma cells via regulation of the PI3K/Akt/mTOR pathway: in vitro and in vivo studies. *Int J Mol Med* 2018;42:811–820.
10. Sahu BD, Kalvala AK, Koneru M, et al. Ameliorative effect of fisetin on cisplatin-induced nephrotoxicity in rats via modulation of NF-κB activation and antioxidant defence. *PLoS One* 2014;9:e105070.
11. Ren Q, Tao S, Guo F, et al. Natural flavonol fisetin attenuated hyperuricemic nephropathy via inhibiting IL-6/JAK2/STAT3 and TGF-β/SMAD3 signaling. *Phytomedicine* 2021;87:153552.
12. Han SJ, Noh MR, Jung JM, et al. Hydrogen sulfide-producing cystathionine γ-lyase is critical in the progression of kidney fibrosis. *Free Radic Biol Med* 2017;112:423–432.
13. Li Z, Wang Y, Zhang Y, et al. Protective effects of fisetin on hepatic ischemia-reperfusion injury through alleviation of apoptosis and oxidative stress. *Arch Med Res* 2021;52:163–173.
14. Ren Q, Guo F, Tao S, Huang R, Ma L, Fu P. Flavonoid fisetin alleviates kidney inflammation and apoptosis via inhibiting Src-mediated NF-κB p65 and MAPK signaling pathways in septic AKI mice. *Biomed Pharmacother* 2020;122:109772.
15. Zhang L, Tong X, Huang J, et al. Fisetin alleviated bleomycin-induced pulmonary fibrosis partly by rescuing alveolar epithelial cells from senescence. *Front Pharmacol* 2020;11:553690.
16. Meng XM, Tang PM, Li J, Lan HY. TGF-β/Smad signaling in renal fibrosis. *Front Physiol* 2015;6:82.
17. Peng H, Xian D, Liu J, Pan S, Tang R, Zhong J. Regulating the polarization of macrophages: a promising approach to vascular dermatosis. *J Immunol Res* 2020;2020:8148272.
18. Martínez-Klimova E, Aparicio-Trejo OE, Tapia E, Pedraza-Chaverri J. Unilateral ureteral obstruction as a model to investigate fibrosis-attenuating treatments. *Biomolecules* 2019;9:141.
19. Heldin CH, Miyazono K, ten Dijke P. TGF-beta signalling from cell membrane to nucleus through SMAD proteins. *Nature* 1997;390:465–471.
20. Walton KL, Johnson KE, Harrison CA. Targeting TGF-β mediated SMAD signaling for the prevention of fibrosis. *Front Pharmacol* 2017;8:461.
21. Inazaki K, Kanamaru Y, Kojima Y, et al. Smad3 deficiency attenuates renal fibrosis, inflammation, and apoptosis after unilateral ureteral obstruction. *Kidney Int* 2004;66:597–604.
22. Ai J, Nie J, He J, et al. GQ5 hinders renal fibrosis in obstructive nephropathy by selectively inhibiting TGF-β-induced Smad3 phosphorylation. *J Am Soc Nephrol* 2015;26:1827–1838.
23. Chen H, Yang T, Wang MC, Chen DQ, Yang Y, Zhao YY. Novel RAS inhibitor 25-O-methylalisol F attenuates epithelial-to-mesenchymal transition and tubulo-interstitial fibrosis by selectively inhibiting TGF-β-mediated Smad3 phosphorylation. *Phytomedicine* 2018;42:207–218.
24. Liu L, Gan S, Li B, Ge X, Yu H, Zhou H. Fisetin alleviates atrial inflammation, remodeling, and vulnerability to atrial fibrillation after myocardial infarction. *Int Heart J* 2019;60:1398–1406.
25. Aranda-Rivera AK, Cruz-Gregorio A, Aparicio-Trejo OE, Ortega-Lozano AJ, Pedraza-Chaverri J. Redox signaling pathways in unilateral ureteral obstruction (UUO)-induced renal fibrosis. *Free Radic Biol Med* 2021;172:65–81.
26. Mittal M, Siddiqui MR, Tran K, Reddy SP, Malik AB. Reactive oxygen species in inflammation and tissue injury. *Antioxid Redox Signal* 2014;20:1126–1167.
27. Moriyama T, Kawada N, Nagatoya K, Horio M, Imai E, Hori M. Oxidative stress in tubulointerstitial injury: therapeutic potential of antioxidants towards interstitial fibrosis. *Nephrol Dial Transplant* 2000;15 Suppl 6:47–49.
28. Qing X, Shi D, Lv X, Wang B, Chen S, Shao Z. Prognostic significance of 8-hydroxy-2'-deoxyguanosine in solid tumors: a meta-analysis. *BMC Cancer* 2019;19:997.
29. Milkovic L, Cipak Gasparovic A, Zarkovic N. Overview on major lipid peroxidation bioactive factor 4-hydroxynonenal as pluripotent growth-regulating factor. *Free Radic Res* 2015;49:850–860.
30. Tamura M, Aizawa R, Hori M, Ozaki H. Progressive renal dysfunction and macrophage infiltration in interstitial fibrosis in an adenine-induced tubulointerstitial nephritis mouse model. *Histochem Cell Biol* 2009;131:483–490.

31. Shen B, Liu X, Fan Y, Qiu J. Macrophages regulate renal fibrosis through modulating TGFβ superfamily signaling. *Inflammation* 2014;37:2076–2084.
32. Fortini F, Vieceli Dalla Sega F, Marracino L, et al. Well-known and novel players in endothelial dysfunction: updates on a Notch(ed) landscape. *Biomedicines* 2021;9:997.
33. Qin CC, Liu YN, Hu Y, Yang Y, Chen Z. Macrophage inflammatory protein-2 as mediator of inflammation in acute liver injury. *World J Gastroenterol* 2017;23:3043–3052.
34. Kaneko N, Kurata M, Yamamoto T, Morikawa S, Masumoto J. The role of interleukin-1 in general pathology. *Inflamm Regen* 2019;39:12.
35. Ashcroft GS, Yang X, Glick AB, et al. Mice lacking Smad3 show accelerated wound healing and an impaired local inflammatory response. *Nat Cell Biol* 1999;1:260–266.
36. Pan B, Liu G, Jiang Z, Zheng D. Regulation of renal fibrosis by macrophage polarization. *Cell Physiol Biochem* 2015;35:1062–1069.
37. Tang WB, Ling GH, Sun L, Liu FY. Smad anchor for receptor activation (SARA) in TGF-beta signaling. *Front Biosci (Elite Ed)* 2010;2:857–860.